

## Structural and reactivity comparison of analogous organometallic Pd(III) and Pd(IV) complexes†

Fengzhi Tang,<sup>a</sup> Fengrui Qu,<sup>a</sup> Julia R. Khusnutdinova,<sup>a</sup> Nigam P. Rath<sup>b</sup> and Liviu M. Mirica\*<sup>a</sup>

Received 14th September 2012, Accepted 3rd October 2012

DOI: 10.1039/c2dt32127k

The tetradentate ligands <sup>R</sup>N4 (<sup>R</sup>N4 = *N,N'*-di-alkyl-2,11-diaza[3,3](2,6)pyridinophane, R = Me or *i*Pr) were found to stabilize cationic (<sup>R</sup>N4)Pd<sup>III</sup>Me<sub>2</sub> and (<sup>R</sup>N4)Pd<sup>III</sup>MeCl complexes in both Pd<sup>III</sup> and Pd<sup>IV</sup> oxidation states. This allows for the first time a direct structural and reactivity comparison of the two Pd oxidation states in an identical ligand environment. The Pd<sup>III</sup> complexes exhibit a distorted octahedral geometry, as expected for a d<sup>7</sup> metal center, and display unselective C–C and C–Cl bond formation reactivity. By contrast, the Pd<sup>IV</sup> complexes have a pseudo-octahedral geometry and undergo selective non-radical C–C or C–Cl bond formation that is controlled by the ability of the complex to access a five-coordinate intermediate.

## Introduction

The role of Pd<sup>0</sup>/Pd<sup>II</sup> intermediates in palladium-catalyzed reactions has been studied extensively for the past four decades.<sup>1</sup> In addition, Pd<sup>IV</sup> and Pd<sup>III</sup> complexes have recently been proposed as catalytically active intermediates in various oxidative organic transformations that complement the conventional Pd<sup>0/II</sup> catalysis.<sup>2</sup> In this context, development of ligand systems that can stabilize both Pd<sup>III</sup> and Pd<sup>IV</sup> complexes in a similar coordination environment can provide key insight into the mechanism of these important catalytic transformations,<sup>3</sup> especially for systems in which either one or both oxidation states have been proposed to be responsible for the observed reactivity.<sup>4</sup>

We have recently reported the first mononuclear organometallic Pd<sup>III</sup> complexes – stabilized by a tetradentate ligand *N,N'*-di-*tert*-butyl-2,11-diaza[3,3](2,6)pyridinophane (<sup>t</sup>BuN4), and studied their C–C bond formation reactivity.<sup>5</sup> We have also investigated the involvement of Pd<sup>III</sup> species in aerobically-induced C–C bond formation from Pd<sup>II</sup> precursors<sup>6</sup> and in Kharasch radical additions.<sup>7</sup> Continuing our study of high valent Pd chemistry, herein we report the use of *N*-methyl (<sup>Me</sup>N4) and *N*-isopropyl (<sup>i</sup>PrN4) pyridinophane ligand analogs that lead to the

isolation and characterization of analogous mononuclear Pd<sup>III</sup> and Pd<sup>IV</sup> complexes. Isolation of these complexes enabled a direct structural and reactivity comparison of the two Pd oxidation states in an identical ligand environment.

## Results and discussion

Synthesis and properties of Pd<sup>III</sup> and Pd<sup>IV</sup> complexes

The <sup>Me</sup>N4 and <sup>i</sup>PrN4 ligands were synthesized using reported and slightly modified synthetic procedures<sup>8</sup> and were used to prepare the Pd<sup>II</sup> precursors (<sup>Me</sup>N4)Pd<sup>II</sup>MeCl (**1**), (<sup>i</sup>PrN4)Pd<sup>II</sup>MeCl (**2**), (<sup>Me</sup>N4)Pd<sup>II</sup>Me<sub>2</sub> (**3**), and (<sup>i</sup>PrN4)Pd<sup>II</sup>Me<sub>2</sub> (**4**) (Scheme 1).<sup>9</sup> Cyclic voltammetry (CV) studies of complexes **1–4** in MeCN reveal two oxidation waves assigned to Pd<sup>II</sup>/Pd<sup>III</sup> and Pd<sup>III</sup>/Pd<sup>IV</sup> redox couples, respectively (Fig. 1 and Table 1).<sup>5,9,10</sup> Interestingly, these oxidation potentials increase with the increasing steric bulk of the ligand from <sup>Me</sup>N4 to <sup>i</sup>PrN4 to <sup>t</sup>BuN4. For example, the

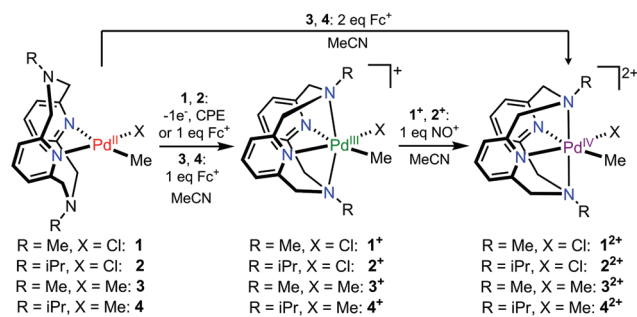
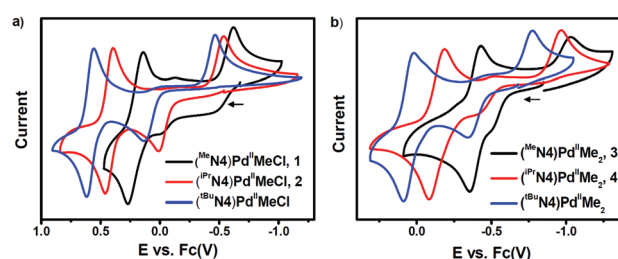
Scheme 1 Synthesis of (<sup>R</sup>N4)Pd<sup>III</sup> and (<sup>R</sup>N4)Pd<sup>IV</sup> complexes.

Fig. 1 CVs of (a) <sup>R</sup>N4Pd<sup>III</sup>MeCl and (b) <sup>R</sup>N4Pd<sup>III</sup>Me<sub>2</sub> complexes. Conditions: 0.1 M Bu<sub>4</sub>NClO<sub>4</sub>–MeCN or CH<sub>2</sub>Cl<sub>2</sub>, 100 mV s<sup>-1</sup>. The CV data for [(<sup>t</sup>BuN4)Pd<sup>III</sup>MeCl]<sup>+</sup> were taken from ref. 5.

<sup>a</sup>Department of Chemistry, Washington University, One Brookings Drive, St. Louis, Missouri 63130-489, USA. E-mail: mirica@wustl.edu

<sup>b</sup>Department of Chemistry and Biochemistry, University of Missouri–St. Louis, One University Boulevard, St. Louis, Missouri 63121-4400, USA

† Electronic supplementary information (ESI) available. CCDC 884994. For ESI and crystallographic data in CIF or other electronic format see DOI: 10.1039/c2dt32127k

**Table 1** Spectroscopic properties of Pd<sup>III</sup> complexes

	$E_{pc}^{III/II}$ , $E_{pa}^{II/III}$ , $E_{1/2}^{III/IV}$ ( $\Delta E_p$ ) <sup>a</sup> (mV)	UV-vis (MeCN), $\lambda$ (nm) ( $\epsilon$ , M <sup>-1</sup> cm <sup>-1</sup> )	EPR, $g_x$ , $g_y$ , $g_z$ ( $A_N$ , G) <sup>b</sup>
<b>1</b> <sup>+</sup>	-620/-135, -480/-20, <sup>c</sup> +205 (130)	606 (615), 475 (480), 316 (3550)	2.212, 2.101, 2.014 (23.0)
<b>2</b> <sup>+</sup>	-535, +10, +428 (65)	658 (810), 517 (580), 312 (4020)	2.228, 2.115, 2.011 (21.3)
<b>A</b> <sup>+d</sup>	-464, +134, +587 (63)	723 (1100), 545 (490), 368 (3300)	2.239, 2.134, 2.005 (19.5)
<b>3</b> <sup>+</sup>	-1030, -520, -395 (75)	620 (405), 490 (430), 365 (1500)	2.168 (16.0), 2.168 (16.0), 1.989 (22.5)
<b>4</b> <sup>+</sup>	-965, -420, -135 (100)	666 (623), 500 (500), 339 (4545)	2.184 (15.0), 2.184 (15.0), 1.988 (20.4)
<b>B</b> <sup>+e</sup>	-774, -341, +53 (67)	741 (360), 560 (160), 350 (2300)	2.222 (12.0), 2.191 (13.8), 1.986 (18.0)

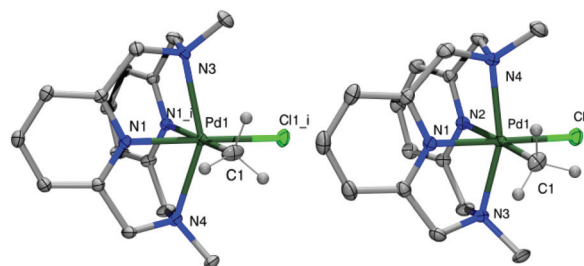
<sup>a</sup> Measured for Pd<sup>II</sup> precursors by CV vs. Fc<sup>+</sup>/Fc in 0.1 M Bu<sub>4</sub>NClO<sub>4</sub>-MeCN or CH<sub>2</sub>Cl<sub>2</sub>, scan rate 100 mV s<sup>-1</sup>;  $\Delta E_p$  is the peak potential separation for the Pd<sup>III/IV</sup> couple. <sup>b</sup> In 3 : 1 PrCN : MeCN, 77 K;  $A_N$ 's are superhyperfine coupling constants to the axial N atoms. <sup>c</sup> The duplicate  $E_{pa}^{II/III}$  and  $E_{pc}^{III/II}$  values are likely due to two conformations present in solution (ref. 5). <sup>d</sup> CV and UV-vis data for [(<sup>t</sup>BuN4)Pd<sup>III</sup>MeCl]<sup>+</sup> (**A**<sup>+</sup>) are from ref. 5. <sup>e</sup> UV-vis and EPR data for [(<sup>t</sup>BuN4)Pd<sup>III</sup>Me<sub>2</sub>]<sup>+</sup> (**B**<sup>+</sup>) are from refs. 5 and 6, respectively.

$E_{1/2}^{III/IV}$  values of Me<sub>4</sub>N complexes **1** and **3** are ~400 mV lower than those for the analogous <sup>t</sup>BuN4Pd<sup>II</sup> complexes (Table 1).<sup>5</sup> The presence of such low Pd<sup>III/IV</sup> oxidation potentials and an appreciable separation between the Pd<sup>II/III</sup> and Pd<sup>III/IV</sup> potentials suggest that both Pd<sup>III</sup> and Pd<sup>IV</sup> species can be stabilized by Me<sub>4</sub>N4 and <sup>i</sup>PrN4 (*vide infra*).

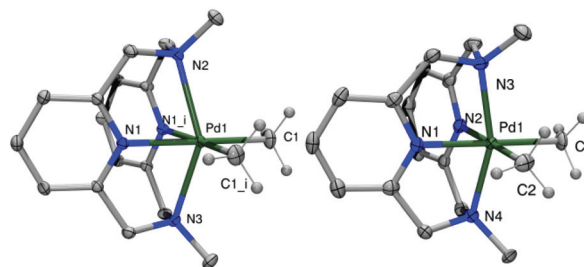
One-electron oxidation of <sup>R</sup>N4Pd<sup>II</sup>MeCl complexes **1** and **2** by controlled potential electrolysis (CPE) in 0.1 M Bu<sub>4</sub>NClO<sub>4</sub>-MeCN or chemical oxidation with 1 equiv. ferrocenium hexafluorophosphate (Fc<sup>+</sup>PF<sub>6</sub><sup>-</sup>) generate the Pd<sup>III</sup> species [(<sup>Me</sup>N4)Pd<sup>III</sup>MeCl]<sup>+</sup> (**1**<sup>+</sup>) and [(<sup>i</sup>PrN4)Pd<sup>III</sup>MeCl]<sup>+</sup> (**2**<sup>+</sup>), while oxidation of **3** and **4** with 1 equiv. Fc<sup>+</sup>PF<sub>6</sub><sup>-</sup> yields [(<sup>Me</sup>N4)Pd<sup>III</sup>Me<sub>2</sub>]<sup>+</sup> (**3**<sup>+</sup>) and [(<sup>i</sup>PrN4)Pd<sup>III</sup>Me<sub>2</sub>]<sup>+</sup> (**4**<sup>+</sup>), respectively (Scheme 1).<sup>9</sup> The X-ray structures of [**1**<sup>+</sup>]<sup>+</sup>ClO<sub>4</sub><sup>-</sup>, [**2**<sup>+</sup>]<sup>+</sup>ClO<sub>4</sub><sup>-</sup>, [**3**<sup>+</sup>]<sup>+</sup>ClO<sub>4</sub><sup>-</sup>, and [**4**<sup>+</sup>]<sup>+</sup>ClO<sub>4</sub><sup>-</sup> all reveal the presence of the expected distorted octahedral geometry at the d<sup>7</sup> Pd<sup>III</sup> center (Fig. 2–4 and S33†).<sup>10,11</sup> Moreover, the Pd–N<sub>axial</sub> distances increase in ~0.05 Å steps when going from Me<sub>4</sub>N4 to <sup>i</sup>PrN4 to <sup>t</sup>BuN4 due to the increasing steric clash between the N-substituents and the equatorial ligands, as can be observed in the space filling models of the Pd<sup>III</sup> complexes (Fig. S33–S34). The presence of the less bulky N-substituent also leads to a more symmetric structure for the Pd<sup>III</sup> complexes. For example, while **3**<sup>+</sup> exhibits a more symmetric C<sub>2v</sub> geometry, **4**<sup>+</sup> has a C<sub>2</sub> symmetry due to the bulkier <sup>i</sup>PrN4 ligand.<sup>9</sup>

The EPR spectra of complexes **1**<sup>+</sup>–**4**<sup>+</sup> reveal anisotropic signals corresponding to Pd<sup>III</sup> centers with a d<sub>z<sup>2</sup></sub> ground state, as expected for a d<sup>7</sup> ion (Table 1, Fig. S28–S32†).<sup>5,6,9,10</sup> This is further supported by the presence of superhyperfine coupling to the two axial N atoms ( $A_N = 12$ –23 G) that are observed in glassing solvent mixtures at 77 K.<sup>9</sup> Interestingly, the shorter Pd–N<sub>axial</sub> distances due to the size of the N-substituents are also responsible for the increasing trend in the  $A_N$  superhyperfine coupling constants from <sup>t</sup>BuN4 to <sup>i</sup>PrN4 to Me<sub>4</sub>N4 (Table 1), suggesting that these EPR parameters can be used to approximate the strength of Pd–N<sub>axial</sub> interactions in Pd<sup>III</sup> complexes.<sup>9</sup> In addition, the same ligand steric effects likely lead to a red shift of the visible absorption bands with the increasing size of the N-substituent in [(<sup>R</sup>N4)Pd<sup>III</sup>MeCl]<sup>+</sup> and [(<sup>R</sup>N4)Pd<sup>III</sup>Me<sub>2</sub>]<sup>+</sup> complexes (Table 1 and Fig. S23–S24†).<sup>12</sup>

Further chemical oxidation of **1**<sup>+</sup> and **2**<sup>+</sup> with 1 equiv. nitrosium tetrafluoroborate (NO<sup>+</sup>BF<sub>4</sub><sup>-</sup>) in MeCN generates [(<sup>Me</sup>N4)Pd<sup>IV</sup>MeCl]<sup>2+</sup> (**1**<sup>2+</sup>) and [(<sup>i</sup>PrN4)Pd<sup>IV</sup>MeCl]<sup>2+</sup> (**2**<sup>2+</sup>), while treatment of **3** and **4** with 2 equiv. Fc<sup>+</sup>PF<sub>6</sub><sup>-</sup> yields the Pd<sup>IV</sup> complexes [(<sup>Me</sup>N4)Pd<sup>IV</sup>Me<sub>2</sub>]<sup>2+</sup> (**3**<sup>2+</sup>) and [(<sup>i</sup>PrN4)Pd<sup>IV</sup>Me<sub>2</sub>]<sup>2+</sup> (**4**<sup>2+</sup>)



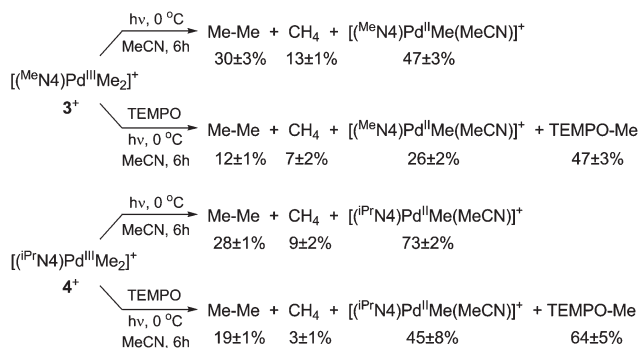
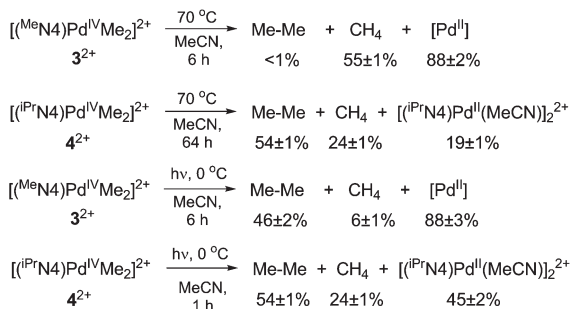
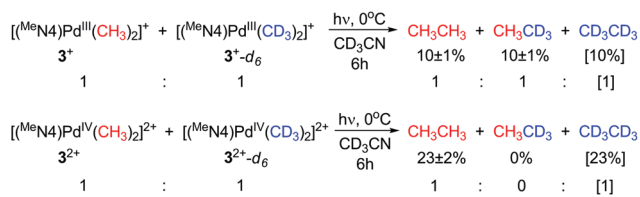
**Fig. 2** ORTEP representation (50% probability ellipsoids) of the cations of [**1**<sup>+</sup>]<sup>+</sup>ClO<sub>4</sub><sup>-</sup> (left) and [**2**<sup>+</sup>]<sup>+</sup>(ClO<sub>4</sub>)<sub>2</sub><sup>-</sup> (right). Selected bond distances (Å) and angles (°): [**1**<sup>+</sup>]<sup>+</sup>ClO<sub>4</sub><sup>-</sup>, Pd1–C1 2.021(1), Pd1–Cl1i 2.344(3), Pd1–N1 2.085(2), Pd1–N1i 2.085(2), Pd1–N3 2.302(3), Pd1–N4 2.338(3), N3–Pd1–N4 149.12(1); [**2**<sup>+</sup>]<sup>+</sup>(ClO<sub>4</sub>)<sub>2</sub><sup>-</sup>, Pd1–C1 2.072(2), Pd1–Cl1 2.2917(6), Pd1–N1 1.966(2), Pd1–N2 2.063(2), Pd1–N3 2.098(2), Pd1–N4 2.105(2), N3–Pd1–N4 158.94(7).



**Fig. 3** ORTEP representation (50% probability ellipsoids) of the cations of [**3**<sup>+</sup>]<sup>+</sup>ClO<sub>4</sub><sup>-</sup> (left) and [**3**<sup>2+</sup>]<sup>+</sup>(PF<sub>6</sub>)<sub>2</sub><sup>-</sup> (right). Selected bond distances (Å) and angles (°): [**3**<sup>+</sup>]<sup>+</sup>ClO<sub>4</sub><sup>-</sup>, Pd1–C1 2.0432(10), Pd1–Cl1i 2.0433(10), Pd1–N1 2.1393(7), Pd1–N1i 2.1393(7), Pd1–N2 2.4013(11), Pd1–N3 2.3506(12), N2–Pd1–N3 145.37(4); [**3**<sup>2+</sup>]<sup>+</sup>(PF<sub>6</sub>)<sub>2</sub><sup>-</sup>, Pd1–C1 2.042(3), Pd1–C2 2.039(3), Pd1–N1 2.054(2), Pd1–N2 2.058(3), Pd1–N3 2.129(3), Pd1–N4 2.116(2), N3–Pd1–N4 156.70(10).

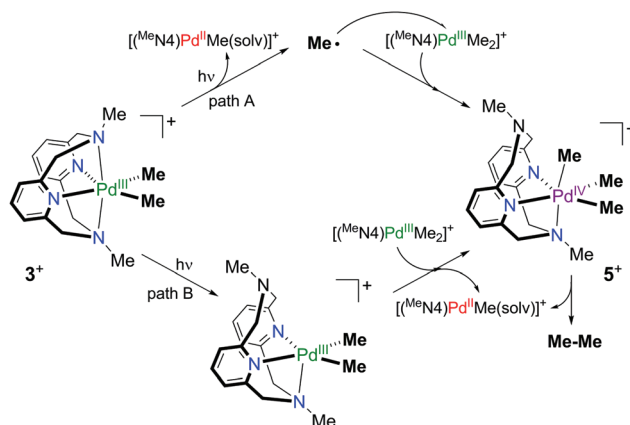
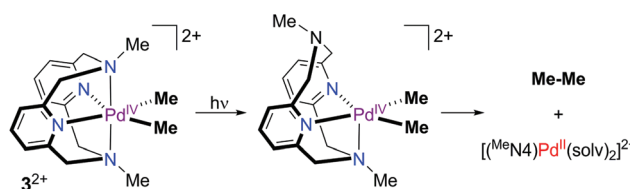
(Scheme 1).<sup>9</sup> The X-ray structures of [**1**<sup>2+</sup>]<sup>+</sup>(ClO<sub>4</sub>)<sub>2</sub><sup>-</sup>, [**3**<sup>2+</sup>]<sup>+</sup>(PF<sub>6</sub>)<sub>2</sub><sup>-</sup>, and [**4**<sup>2+</sup>]<sup>+</sup>(PF<sub>6</sub>)<sub>2</sub><sup>-</sup> confirm the presence of Pd<sup>IV</sup> centers with a pseudo-octahedral geometry and reveal Pd–N<sub>axial</sub> distances that are 0.24–0.27 Å shorter than those in the Pd<sup>III</sup> analogs **1**<sup>+</sup>, **3**<sup>+</sup>, and **4**<sup>+</sup>, respectively (Fig. 2–4), in line with the preferred octahedral geometry for a d<sup>6</sup> Pd<sup>IV</sup> center vs. the distorted geometry of a d<sup>7</sup> Pd<sup>III</sup> ion.<sup>10,11</sup> Moreover, the Me<sub>4</sub>N4 ligand can easily accommodate the shorter Pd–N<sub>axial</sub> distances and the more compact structure of the octahedral Pd<sup>IV</sup> centers, as seen in the



Scheme 4 Reactivity of  $[(^{\text{R}}\text{N4})\text{Pd}^{\text{III}}\text{Me}_2]^+$  complexes.<sup>19</sup>Scheme 5 Reactivity of  $[(^{\text{R}}\text{N4})\text{Pd}^{\text{IV}}\text{Me}_2]^{2+}$  complexes.<sup>19</sup>Scheme 6 Crossover experiments for the photolysis of **3<sup>+</sup>** and **3<sup>2+</sup>**.

$\text{Pd}^{\text{IV}}\text{Me}_2]^{2+}$ , which is likely to undergo facile reductive elimination (*vide infra*).<sup>18,20</sup>

Crossover experiments were performed to gain insight into the possible mechanisms of ethane formation in the photolysis of  $[(^{\text{R}}\text{N4})\text{Pd}^{\text{III}}(\text{Me})_2]^+$  and  $[(^{\text{R}}\text{N4})\text{Pd}^{\text{IV}}(\text{Me})_2]^{2+}$  complexes. Photolysis of a 1 : 1 mixture of  $[(^{\text{Me}}\text{N4})\text{Pd}^{\text{III}}(\text{CH}_3)_2]\text{ClO}_4$ , **3<sup>+</sup>**ClO<sub>4</sub>, and  $[(^{\text{Me}}\text{N4})\text{Pd}^{\text{III}}(\text{CD}_3)_2]^+$ , **3<sup>+-d6</sup>**ClO<sub>4</sub>, leads to formation of both CH<sub>3</sub>CH<sub>3</sub> and CH<sub>3</sub>CD<sub>3</sub> in 10% yield. Given the typical yield of ~30% ethane upon photolysis of **3<sup>+</sup>**ClO<sub>4</sub> under the same conditions, the result suggests a CH<sub>3</sub>CH<sub>3</sub> : CH<sub>3</sub>CD<sub>3</sub> : CD<sub>3</sub>CD<sub>3</sub> ratio of 1 : 1 : 1 (Scheme 6). The observed ratio of ethane isotopologs is consistent with the formation of a  $[(\kappa^3\text{-Me}_3\text{N4})\text{Pd}^{\text{IV}}\text{Me}_3]^+$  intermediate (**5<sup>+</sup>**) that undergoes a fast rearrangement of the Me groups and thus can reductively eliminate any two of three Me groups.<sup>6</sup> In addition, the 1 : 1 : 1 ratio does not support a radical mechanism involving the coupling of two Me radicals or an S<sub>H</sub>2-like mechanism involving a Me radical attacking the Me group of another Pd<sup>III</sup>-Me molecule, as these mechanisms would lead to a 1 : 2 : 1 statistical ratio of ethane isotopologs.<sup>21</sup> The proposed intermediate **5<sup>+</sup>** can be generated through a radical

Scheme 7 Proposed mechanisms for the photo-induced ethane elimination from **3<sup>+</sup>** (and **4<sup>+</sup>**).Scheme 8 Proposed mechanism for the photo-induced ethane elimination from **3<sup>2+</sup>** (and **4<sup>2+</sup>**).

mechanism involving a homolytic cleavage of a Pd<sup>III</sup>-Me bond to form a Me radical that can subsequently bind to the Pd<sup>III</sup> center of another molecule of **3<sup>+</sup>** (Scheme 7, path A).<sup>5</sup> Alternatively, a non-radical dissociation of an axial Pd<sup>III</sup>-N<sub>axial</sub> bond upon irradiation can form a transient intermediate  $[(\kappa^3\text{-Me}_3\text{N4})\text{Pd}^{\text{IV}}\text{Me}_3]^+$ , which can undergo Me group transfer *via* disproportionation with another molecule of **3<sup>+</sup>** to yield **5<sup>+</sup>** (Scheme 7, path B).<sup>6,22</sup> The partial suppression of ethane formation by TEMPO suggests that both mechanisms may be operative during photolysis and can generate species **5<sup>+</sup>**, which is responsible for ethane formation.<sup>22</sup>

Interestingly, crossover studies for the Pd<sup>IV</sup> complexes yield different results. Photolysis of a 1 : 1 mixture of  $[(^{\text{Me}}\text{N4})\text{Pd}^{\text{IV}}(\text{CH}_3)_2](\text{PF}_6)_2$ , **3<sup>2+</sup>**(PF<sub>6</sub>)<sub>2</sub>, and  $[(^{\text{Me}}\text{N4})\text{Pd}^{\text{IV}}(\text{CD}_3)_2](\text{PF}_6)_2$ , **3<sup>2+-d6</sup>**(PF<sub>6</sub>)<sub>2</sub>, yields 23% of CH<sub>3</sub>CH<sub>3</sub>, and no crossover product CH<sub>3</sub>CD<sub>3</sub> is formed (Scheme 6).<sup>9</sup> Since the typical yield of ethane upon photolysis of **3<sup>2+</sup>** is ~46%, the result suggests a 1 : 0 : 1 ratio of CH<sub>3</sub>CH<sub>3</sub>, CH<sub>3</sub>CD<sub>3</sub>, and CD<sub>3</sub>CD<sub>3</sub>. The observed ratio is consistent with a non-radical mechanism involving a photo-induced dissociation of an axial N donor to give the 5-coordinate intermediate, followed by rapid concerted reductive elimination of ethane (Scheme 8).<sup>18,20</sup> Overall, these reactivity studies suggest that, by contrast to Pd<sup>III</sup> analogs, the Pd<sup>IV</sup> complexes undergo selective C-C and C-heteroatom bond formation that most likely involve non-radical mechanisms.

## Conclusion

In summary, we have successfully isolated and characterized analogous organometallic Pd<sup>III</sup> and Pd<sup>IV</sup> complexes stabilized by

the tetradentate ligands  $^{\text{Mc}}\text{N4}$  and  $^{\text{Pr}}\text{N4}$ . The unprecedented isolation of both  $\text{Pd}^{\text{III}}$  and  $\text{Pd}^{\text{IV}}$  complexes with an identical ligand environment allowed a direct structural and organometallic reactivity comparison. The  $d^7$   $\text{Pd}^{\text{III}}$  centers prefer a distorted octahedral geometry, while the  $d^6$   $\text{Pd}^{\text{IV}}$  centers adopt a more compact octahedral geometry. In addition, reactivity studies show that  $\text{Pd}^{\text{III}}$  centers lead to photo-induced radical formation and unselective C–C and C–Cl bond formation, although transient  $\text{Pd}^{\text{IV}}$  intermediates can also be involved. By comparison,  $\text{Pd}^{\text{IV}}$  centers undergo selective C–C or C–Cl bond formation through non-radical reductive elimination mechanisms. Overall, these studies suggest that both  $\text{Pd}^{\text{III}}$  and  $\text{Pd}^{\text{IV}}$  species could act as intermediates in various oxidatively-induced C–C and C–heteroatom bond formation reactions, while  $\text{Pd}^{\text{IV}}$  centers tend to exhibit a more selective and higher yielding reductive elimination reactivity. Our current research efforts aim to provide insight into the involvement of  $\text{Pd}^{\text{III}}$  and/or  $\text{Pd}^{\text{IV}}$  species in stoichiometric and catalytic organic transformations employing high-valent Pd intermediates.

## Notes and references

- (a) E. Negishi, *Handbook of Organopalladium Chemistry for Organic Synthesis*, John Wiley & Sons, Hoboken, NJ, 2002; (b) P. W. N. M. van Leeuwen, *Homogeneous Catalysis: Understanding the Art*, Kluwer Academic Publishers, Dordrecht, 2004; (c) J. F. Hartwig, *Organotransition Metal Chemistry: From Bonding to Catalysis*, University Science Books, Sausalito, 2010.
- (a) A. Canty, *Dalton Trans.*, 2009, 10409; (b) X. Chen, K. M. Engle, D.-H. Wang and J.-Q. Yu, *Angew. Chem., Int. Ed.*, 2009, **48**, 5094; (c) K. Muniz, *Angew. Chem., Int. Ed.*, 2009, **48**, 9412; (d) T. W. Lyons and M. S. Sanford, *Chem. Rev.*, 2010, **110**, 1147; (e) P. Sehnal, R. J. K. Taylor and I. J. S. Fairlamb, *Chem. Rev.*, 2010, **110**, 824; (f) L.-M. Xu, B.-J. Li, Z. Yang and Z.-J. Shi, *Chem. Soc. Rev.*, 2010, **39**, 712; (g) D. C. Powers and T. Ritter, *Top. Organomet. Chem.*, 2011, **35**, 129.
- D. C. Powers, E. Lee, A. Ariafard, M. S. Sanford, B. F. Yates, A. J. Canty and T. Ritter, *J. Am. Chem. Soc.*, 2012, **134**, 12002.
- (a) W.-Y. Yu, W. N. Sit, K.-M. Lai, Z. Zhou and A. S. C. Chan, *J. Am. Chem. Soc.*, 2008, **130**, 3304; (b) T. S. Mei, X. S. Wang and J. Q. Yu, *J. Am. Chem. Soc.*, 2009, **131**, 10806; (c) K. M. Engle, T. S. Mei, X. S. Wang and J. Q. Yu, *Angew. Chem., Int. Ed.*, 2011, **50**, 1478.
- J. R. Khusnutdinova, N. P. Rath and L. M. Mirica, *J. Am. Chem. Soc.*, 2010, **132**, 7303.
- J. R. Khusnutdinova, N. P. Rath and L. M. Mirica, *J. Am. Chem. Soc.*, 2012, **134**, 2414.
- J. R. Khusnutdinova, N. P. Rath and L. M. Mirica, *Angew. Chem., Int. Ed.*, 2011, **50**, 5532.
- (a) F. Bottino, M. Di Grazia, P. Finocchiaro, F. R. Fronczek, A. Mamo and S. Pappalardo, *J. Org. Chem.*, 1988, **53**, 3521; (b) C. M. Che, Z. Y. Li, K. Y. Wong, C. K. Poon, T. C. W. Mak and S. M. Peng, *Polyhedron*, 1994, **13**, 771.
- See ESI†
- L. M. Mirica and J. R. Khusnutdinova, *Coord. Chem. Rev.*, 2012, **256**, DOI: 10.1016/j.ccr.2012.04.030.
- (a) A. J. Blake, A. J. Holder, T. I. Hyde and M. Schröder, *J. Chem. Soc., Chem. Commun.*, 1987, 987; (b) A. J. Blake, L. M. Gordon, A. J. Holder, T. I. Hyde, G. Reid and M. Schröder, *J. Chem. Soc., Chem. Commun.*, 1988, 1452; (c) A. R. Dick, J. W. Kampf and M. S. Sanford, *J. Am. Chem. Soc.*, 2005, **127**, 12790.
- The detailed characterization of the observed spectroscopic trends for complexes  $1^+-4^+$  is ongoing and will be reported elsewhere.
- The  $\text{Pd}^{\text{IV}}$  species  $[(^{\text{tBu}}\text{N4})\text{Pd}^{\text{IV}}\text{MeCl}]^{2+}$  can be generated electrochemically at low temperatures, yet it is unstable at RT (ref. 6).
- Only one other dicationic organometallic complex has been reported to date: W. Oloo, P. Y. Zavalij, J. Zhang, E. Khaskin and A. N. Vedernikov, *J. Am. Chem. Soc.*, 2010, **132**, 14400.
- While a few monoaryl  $\text{Pd}^{\text{IV}}$  complexes have been isolated to date (T. Furuya and T. Ritter, *J. Am. Chem. Soc.*, 2008, **130**, 10060; N. D. Ball and M. S. Sanford, *J. Am. Chem. Soc.*, 2009, **131**, 3796; P. L. Arnold, M. S. Sanford and S. M. Pearson, *J. Am. Chem. Soc.*, 2009, **131**, 13912; Ref. 14), only one other monoalkyl  $\text{Pd}^{\text{IV}}$  complex has been reported: D. Shabashov and O. Daugulis, *J. Am. Chem. Soc.*, 2010, **132**, 3965.
- Thermolysis in the dark of  $\text{Pd}^{\text{III}}$  complexes leads to unspecific decomposition and formation of methane. In addition, photolysis or thermolysis of  $\text{Pd}^{\text{II}}$  precursors leads to formation of methane and Pd black, along with small amounts of ethane or MeCl.
- (a) S. S. Stahl, J. A. Labinger and J. E. Bercaw, *Angew. Chem., Int. Ed.*, 1998, **37**, 2181; (b) B. S. Williams and K. I. Goldberg, *J. Am. Chem. Soc.*, 2001, **123**, 2576.
- (a) J. M. Racowski, A. R. Dick and M. S. Sanford, *J. Am. Chem. Soc.*, 2009, **131**, 10974; (b) J. M. Racowski and M. S. Sanford, *Top. Organomet. Chem.*, 2011, **35**, 61.
- During the reactivity studies for  $^{\text{R}}\text{N4Pd}^{\text{III}}/\text{Pd}^{\text{IV}}$  complexes, the  $^{\text{R}}\text{N4Pd}^{\text{II}}\text{Me}(\text{solvent})$  or  $^{\text{R}}\text{N4Pd}^{\text{II}}(\text{solvent})_2$  products are unstable and lead to formation of methane and other  $\text{Pd}^{\text{II}}$  products (see ESI†).
- (a) J. Procelewska, A. Zahl, G. Liehr, R. van Eldik, N. A. Smythe, B. S. Williams and K. I. Goldberg, *Inorg. Chem.*, 2005, **44**, 7732; (b) D. M. Crumpton and K. I. Goldberg, *J. Am. Chem. Soc.*, 2000, **122**, 962.
- M. P. Lanci, M. S. Remy, W. Kaminsky, J. M. Mayer and M. S. Sanford, *J. Am. Chem. Soc.*, 2009, **131**, 15618.
- We have independently synthesized the  $[(\kappa^3\text{-McN4})\text{Pd}^{\text{IV}}\text{Me}_3]^+$  species  $5^+$  and shown its involvement in aerobically-induced ethane elimination: F. Tang, Y. Zhang, N. P. Rath and L. M. Mirica, *Organometallics*, 2012, **31**, 6690–6696.